Supplementary Information

Collision-induced and complex-mediated roaming dynamics in the H + C_2H_4 → H_2 + C_2H_3 reaction

Yan-Lin Fu[a,b], Xiaoxiao Lu[b], Yong-Chang Han[a,*], Bina Fu[b,*], Dong H. Zhang[b,*], Joel M. Bowman[c,*]

[a]*Department of Physics, Dalian University of Technology, Dalian, China116024*

[b] *State Key Laboratory of Molecular Reaction Dynamics*

and Center for Theoretical and Computational Chemistry,

Dalian Institute of Chemical Physics,

Chinese Academy of Sciences, Dalian, China 116023

[c]*Department of Chemistry and Cherry L. Emerson Center for Scientific Computation,*

Emory University, Atlanta, Georgia 30322, USA

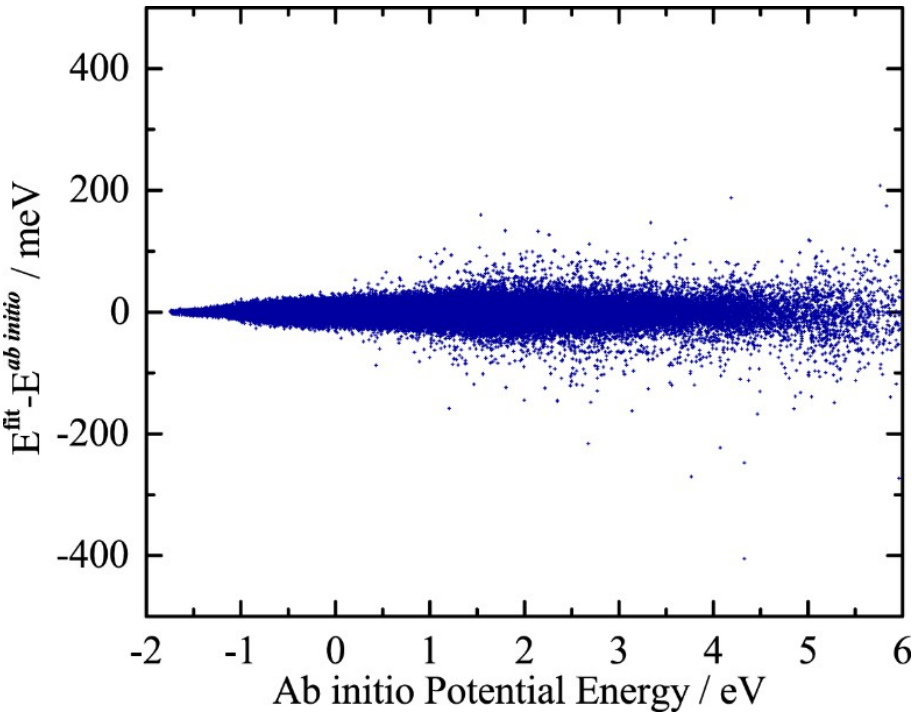

Fig. S1 The fitting errors as a function of their corresponding *ab initio* potential energies of the data points on the FI-NN PES.

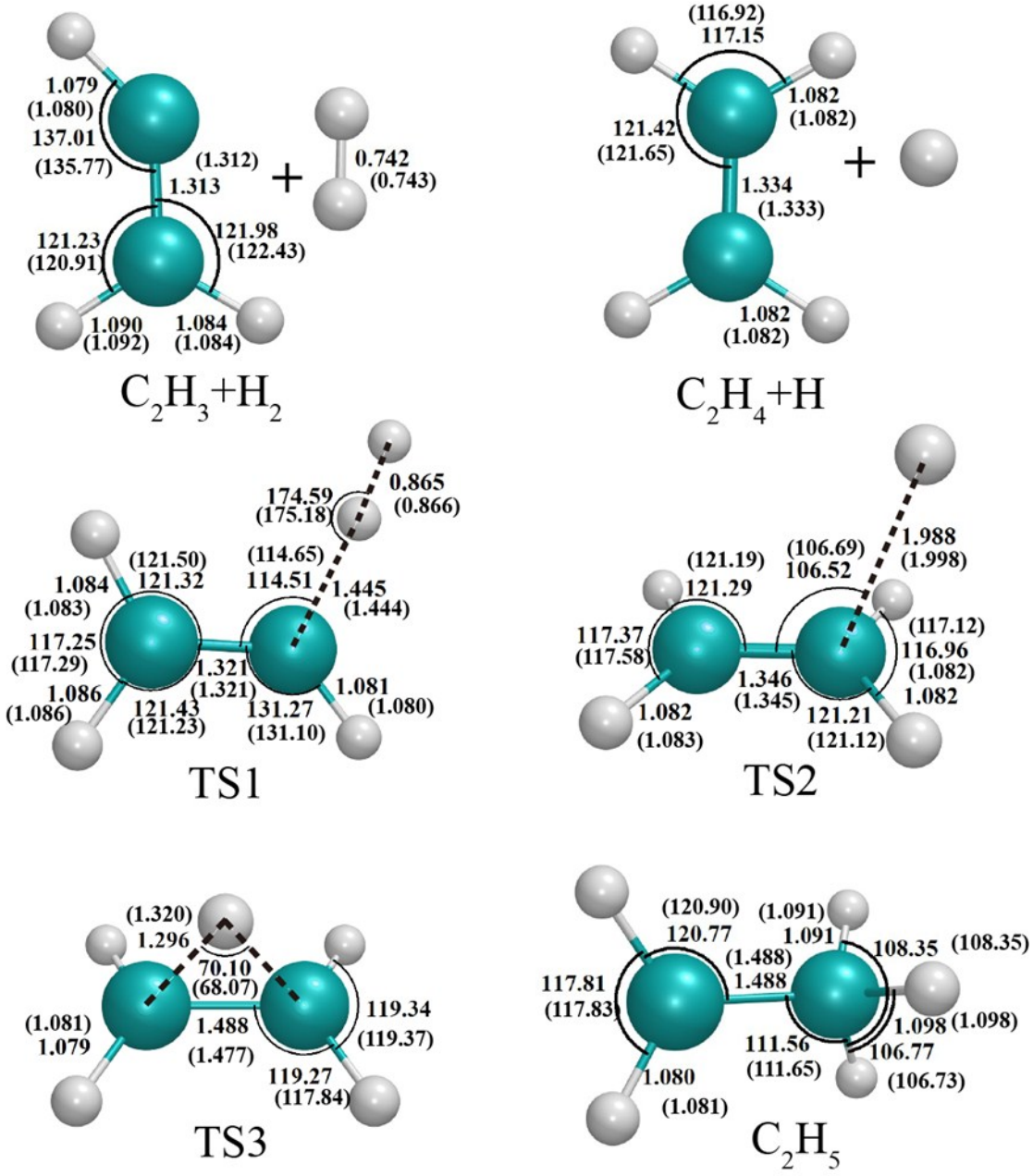

Fig. S2 Optimized geometries (bond lengths in Å, angles in degree) of the reactant species, product species and transition states on the fitted PESs (in parentheses), compared with the results from the UCCSD(T)-F12/AVTZ calculations.

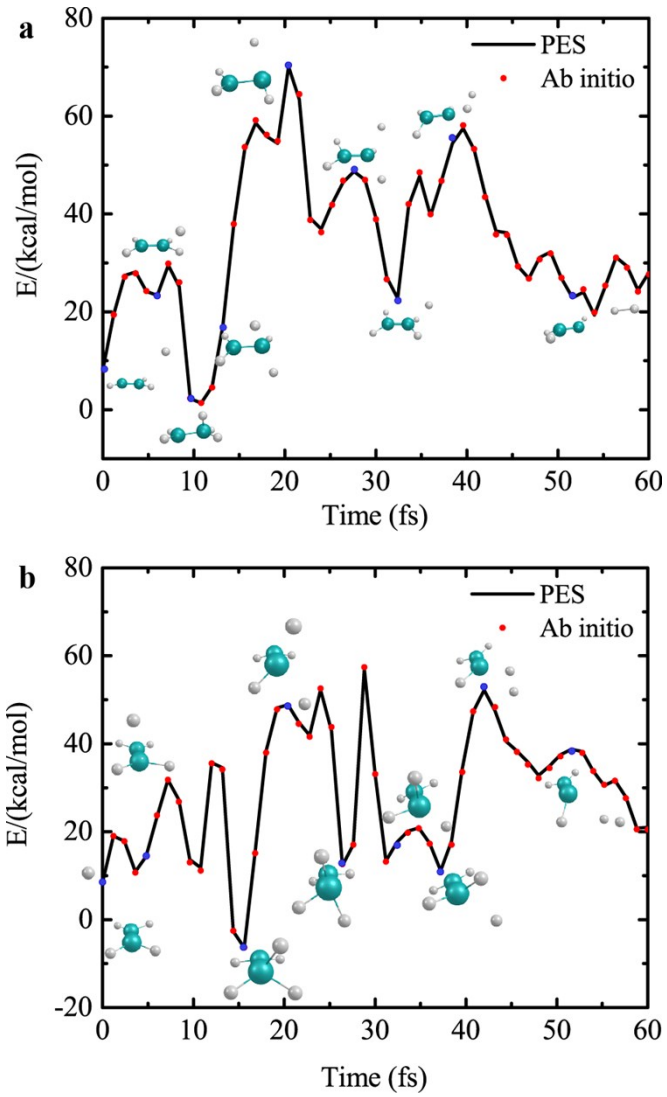

Fig. S3 Comparisons of potential energies between direct UCCSD(T)-F12/AVTZ calculations and fitted results from the FI-NN PES for two representative trajectories with the collision-induced roaming mechanism. (a) backward scattering; (b) forward scattering. Snapshots at selected reaction time are also depicted.

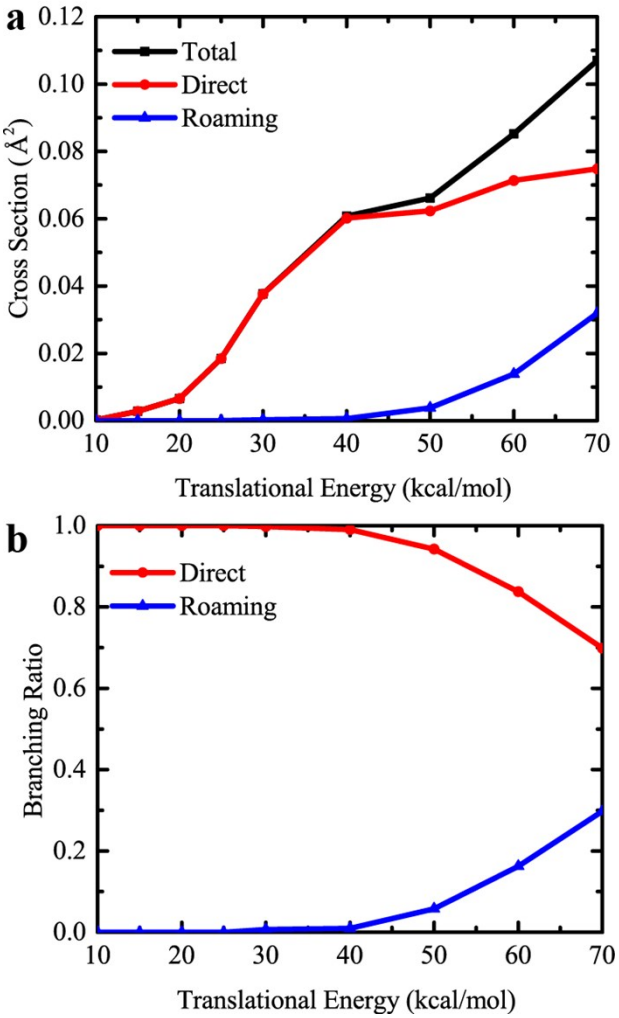

Fig. S4 (a) Cross sections of the direct abstraction and roaming pathways. (b) Same as (a), except for the branching fractions.

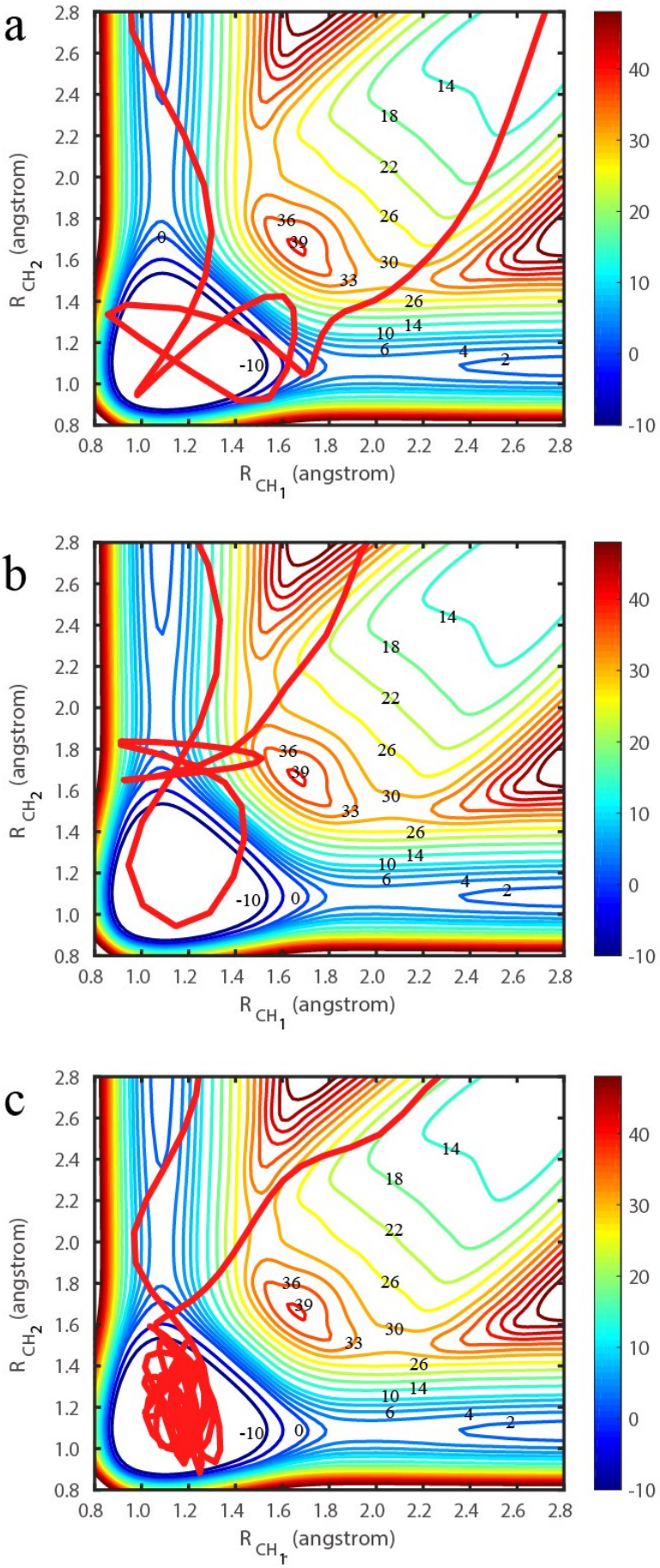
a
b
c
R CH2 (angstrom)
R CH1 (angstrom)
0.8 1.0 1.2 1.4 1.6 1.8 2.0 2.2 2.4 2.6 2.8
40 30 20 10 0 -10
-10
0
2
4
6
10
14
18
22
26
30
33
36
39

Fig. S5 Contour plots of PES as functions of two CH internuclear distances (RCH_1 and RCH_2) of C_2H_5, with other coordinates (degrees of freedom) optimized. Note that roaming occurs when the dihedral φ between the plane of C-C-H_1 and C-C-H_2 larger than 30°, which is quite different from the direct abstraction via TS1(φ around 0°), we restricted this dihedral >30° in the optimization to distinguish the roaming channel from the direct abstraction channel. The evolution of three typical roaming trajectories is also superimposed on the contour plots of PES, namely two collision-induced roaming trajectories (a, b) with extremely short reaction time and a complex-mediated roaming trajectory with long-lived complex (c).

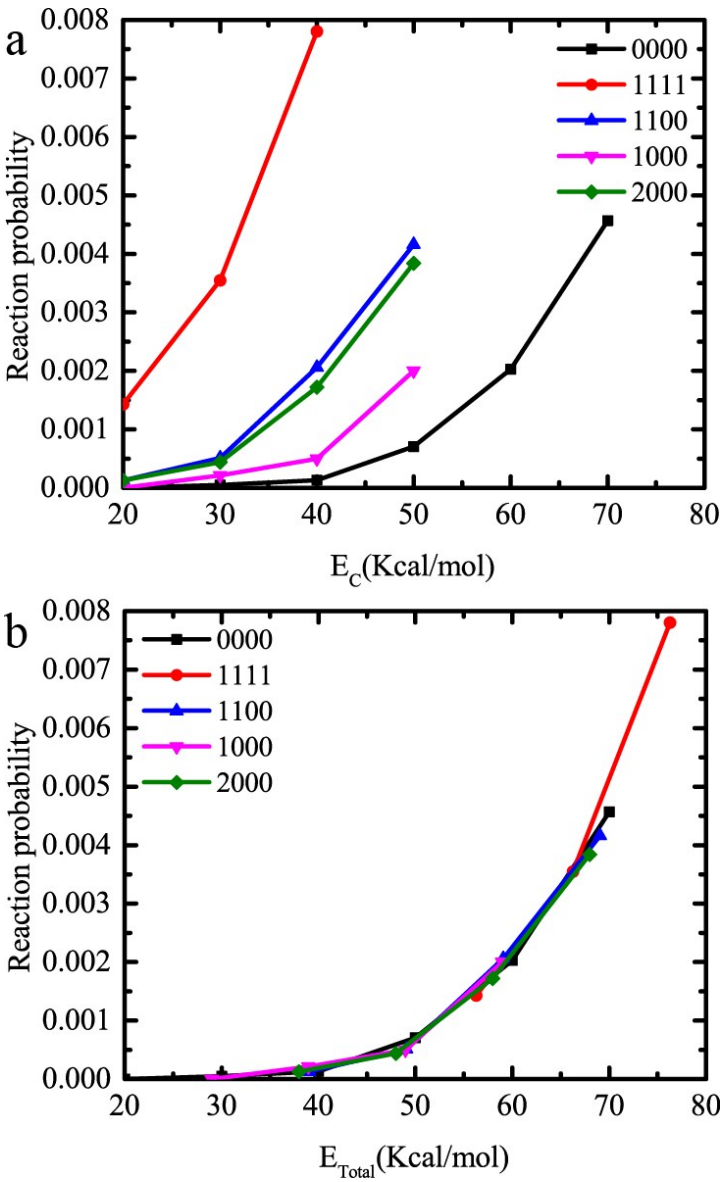

Fig. S6 (a) The reaction probabilities as a function of collision energy of roaming from different vibrational excitations of various modes of C_2H_4, at the impact

parameter b=0. Here, the notations (ν_1, ν_2, ν_3, ν_4) correspond to the symmetric stretch and asymmetric stretch of CH_2 (ν_1 and ν_2), and symmetric and asymmetric stretch of another CH_2 (ν_3 and ν_4) of the reactant C_2H_4. (b) The same as a), except as a function of total energy.

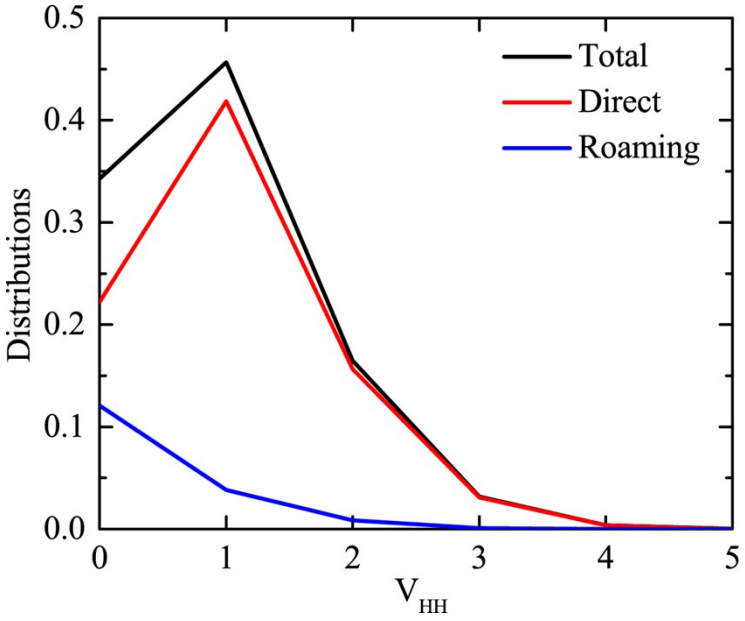

Fig. S7 The final vibrational state distributions of H_2 from the direct abstraction and roaming pathways.

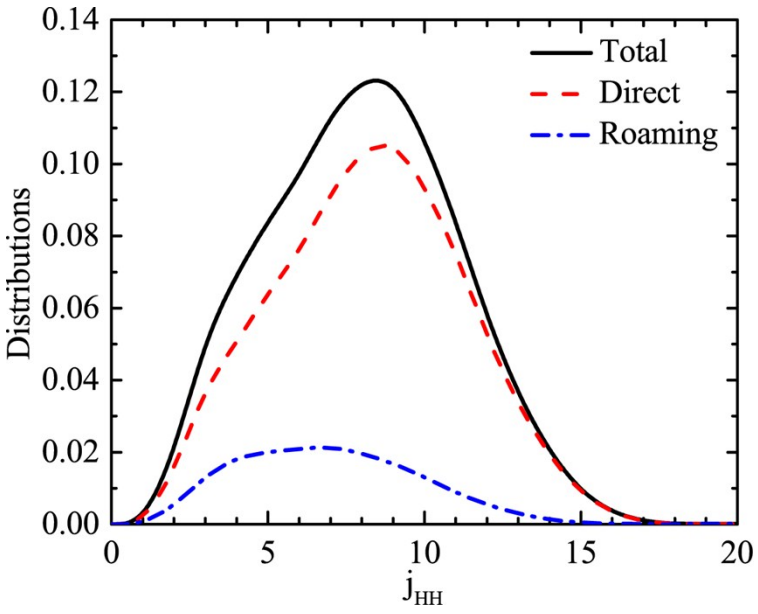

Fig. S8 The final rotational state distributions of H_2 from the direct abstraction and roaming pathways.

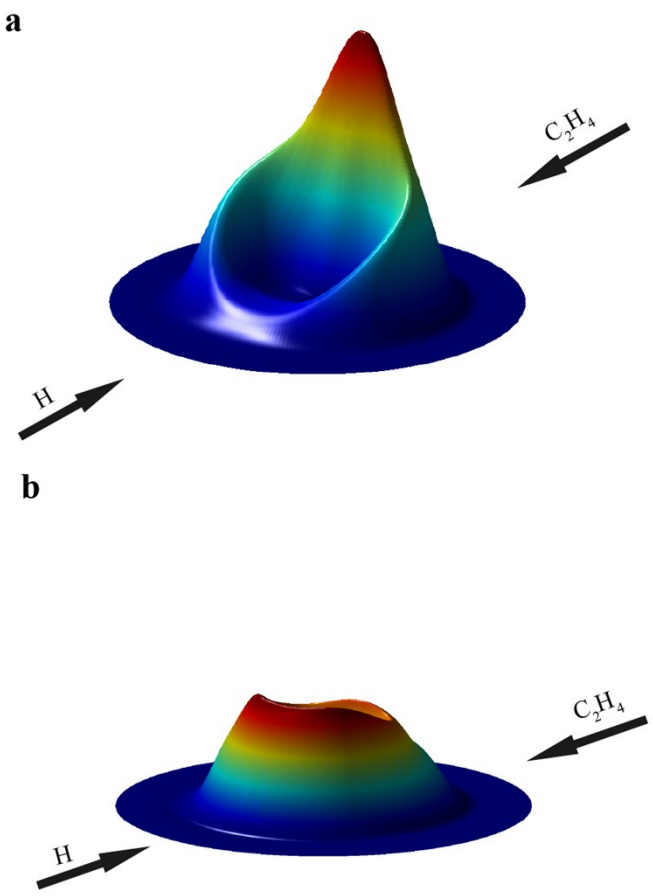

Fig. S9 (a) 3D polar plot for the product translational energy and angular distributions of the H_2 channel from the direct abstraction pathway. Direct abstraction. (b) Same as (a), except for the roaming pathway.

	TS1		TS2		TS3	
	Ab	PES	Ab	PES	Ab	PES
ω_1	*i* 1270.23	*i*1301.29	*i* 704.24	*i* 703.60	*i* 1912.47	*i* 2089.70
ω_2	270.12	263.36	354.49	326.37	564.87	564.12
ω_3	362.14	361.83	389.00	367.60	731.73	609.45
ω_4	813.29	854.26	821.01	832.45	737.89	685.81
ω_5	881.90	875.14	924.13	913.08	781.30	750.50
ω_6	911.74	908.64	980.99	962.55	1132.93	1153.42
ω_7	941.08	946.36	1035.46	1051.75	1194.98	1278.58
ω_8	1071.08	1078.08	1245.47	1259.06	1274.74	1307.37
ω_9	1142.32	1156.00	1338.55	1359.34	1422.61	1364.14
ω_{10}	1395.87	1426.85	1473.72	1453.99	1450.72	1409.77
ω_{11}	1608.39	1604.87	1623.78	1635.55	2222.30	2251.82
ω_{12}	2059.08	2012.38	3144.00	3132.74	3162.40	3046.28
ω_{13}	3108.29	3117.89	3155.71	3154.13	3167.56	3061.88
ω_{14}	3196.35	3192.33	3227.60	3241.63	3272.06	3238.71
ω_{15}	3218.63	3218.63	3252.33	3261.70	3292.13	3270.81

	H_2		C_2H_3		C_2H_4		C_2H_5	
	Ab	PES	Ab	PES	Ab	PES	Ab	PES
ω_1	4400.54	4396.43	714.49	751.47	823.81	837.01	118.64	78.66
ω_2			809.72	835.61	946.00	957.43	470.66	454.05
ω_3			912.60	915.84	964.36	959.58	810.16	802.34
ω_4			1066.16	1050.88	1038.34	1027.43	988.09	987.85
ω_5			1392.16	1424.96	1247.35	1248.26	1072.30	1070.51
ω_6			1616.94	1603.72	1367.68	1374.69	1202.23	1194.49
ω_7			3070.66	3071.35	1476.77	1485.81	1406.41	1407.82
ω_8			3177.07	3182.13	1670.76	1663.95	1477.75	1477.11
ω_9			3247.92	3246.74	3139.98	3119.89	1492.69	1495.69
ω_{10}					3155.42	3147.03	1493.29	1501.47
ω_{11}					3221.66	3217.38	2981.70	2989.17
ω_{12}					3247.64	3223.43	3065.61	3071.82
ω_{13}							3111.35	3107.79
ω_{14}							3157.39	3157.11
ω_{15}							3261.51	3253.76

Table S1 Comparisons of the vibrational frequencies of the transition states (upper) and stationary points (lower) between the results of direct UCCSD(T)-F12a/AVTZ calculations and PES.

Movie S1. Real time video showing the evolution of one collision-induced roaming trajectory, which yields the backward-scattered product.

Movie S2. Real time video showing the evolution of one collision-induced roaming trajectory, which yields the forward-scattered product.

SUPPLEMENTARY METHODs

A. Potential energy surface (PES)

In this work, the spin unrestricted explicitly correlated coupled-cluster method with singles, doubles, and perturbative triples (UCCSD(T)-F12a), together with Dunning's augmented correlation-consistent triple-zeta (aug-cc-pVTZ) basis set has been used to optimize the stationary points and obtain the single-point energies of the data set of the current PES. All the *ab initio* calculations were implemented in the MOLPRO 2012.1.[1,2]A total of 101459 UCCSD(T)-F12a/aug-cc-pVTZ energy points were fitted by the fundamental-invariant neural network (FI-NN) approach. [3,4,5] Considering the possible multi-reference character in some regions of the PES, further T1 diagnostic calculations were carried out to check the reliability and monitor the quality of coupled cluster calculations. A small number of energy points with T1 diagnostic values larger than 0.05 was discarded. Actually we only discarded about 200 data points during the calculations, indicating the reliability of current coupled cluster calculations.

The FI-NN approach uses the fundamental invariants (FIs) as the input vector of NN function, which guarantee the permutational symmetry of the PES. The FIs minimize the size of input invariants and consists of the least number of invariants at a specified truncated or maximum degree. Thus, FI-NN can efficiently reduce the evaluation time of potential energy compared to the corresponding PIP-NN PESs, in particular for larger molecular systems with more identical atoms.[3,4]

The neural network (NN) method is a general fitting method, which is extremely flexible and in principle it can be used to fit any shape of function with very high accuracy.[6] The structure of the feedforward NN is 171-20-40-1, which contains 171 FIs (up to the maximum degree of 5) as the input, 20 and 40 neurons in two hidden layers, and a done output of potential energy.

The functional form we used can be written as:

$$y = b^3 + \sum_{k=1}^{K} \omega_k^3 \cdot f^2\left[b_k^2 + \sum_{j=1}^{J} \omega_{jk}^2 \cdot f^1\left(b_j^1 + \sum_{i=1}^{I} \omega_{ij}^1 \cdot x_i\right)\right] \quad (1)$$

where x_i (i=1,…,I) is the input vector, chosen as 171 FIs here, and y is the output of NN function, corresponding to the potential energy.

In the process of fitting, we get input vectors and corresponding ab initio energies $E_n^{ab\ initio}$ (n = 1,...,N) from a data set containing N points. After evaluating the NN function for each geometry, we get the fitted energies E_n^{fit} (n = 1,...,N). In the FI-NN fitting, roughly 95% of the energy points were selected randomly as the fitting set, while the other 5% of the energy points were left as the validating set. We used the Levenberg-Marquardt algorithm[7] to adjust the parameter of NN, and the fitting quality can be represented by the root mean square error (RMSE):

$$RMSE = \sqrt{\frac{1}{N}\sum_{n=1}^{N}\left(E_n^{ab\ initio} - E_n^{fit}\right)^2} \quad (2)$$

In addition, the "early stopping" method was used to avoid over fitting.[8]

The energy points were selected properly based on direct dynamics simulations and further QCT calculations. The initial 50000 data points were taken from direct dynamic calculations using the unrestricted B3LYP/6-31+g* method, and then further evaluated by the UCCSD(T)-F12a/aug-cc-pVTZ level of theory. Starting from the first PES based on the initial 50000 UCCSD(T)-F12a/aug-cc-pVTZ energies, more energies points were added interactively by performing QCT calculations on those preliminary PESs. Extensive QCT calculations of the $H + C_2H_4$ reaction were carried out to validate the convergence of the fitted PES with respect to the number of energy points. The final FI-NN PES, which is the average of five PESs with minimum RMSEs, results in a RMSE of 13.02 (~0.3 kcal/mol) meV for energies up to 6.0 eV relative to the energy of $H + C_2H_4$.

The PES fits well to the ab initio energies as can be seen from Supplementary Fig. 1, which shows the fitting errors of all data points as a function of their corresponding ab initio energies. This fit results in an overall root mean square error (RMSE) of only 13.7 meV (~0.3 kcal/mol), representing an unprecedented fitting accuracy for PESs of seven-atom multichannel reactions. A comparison of the geometries of the reactant species, product

species and transition states on the fitted PESs and directly from the ab initio UCCSD(T)-F12 calculations is given in Supplementary Figure 2. As shown, the PES describes the stationary points with good accuracy, with the maximum deviation of bond length from UCCSD(T)-F12 results of roughly 1.8% and bond angle of 2.9%. The normal mode frequencies of various species calculated by the UCCSD(T)-F12a/AVTZ method, as well as the corresponding frequencies obtained on the PES are summarized in Supplementary Table 1. The current PES also reproduces well the vibrational frequencies as compared with the direct ab initio calculations.

B. Quasi-classical trajectory calculations

Standard QCT calculations[9,10] for the C_2H_4+H reaction were carried out on our PES with C_2H_4 initially in the ground vibrational state. The quasiclassical ground vibrational state of C_2H_4 was set by randomly sampling the normal coordinates and momenta. The rotational energy of C_2H_4 was sampled form the thermal distribution at 300 K. The initial distance of the H atom from the center of mass of C_2H_4 was $\sqrt{x^2 + b^2}$, where b is the impact parameter and x was set to 6.0 Å. The orientation of C_2H_4 was randomly sampled with respect to the H atom, and b was scanned from 0 to bmax with a step size of 0.2 Å, where b_{max} is the maximum impact parameter. All the trajectories were propagated with a time step of 0.1 fs for a maximum time of 50 ps, using the velocity-Verlet integration scheme, with conserved energies within 0.03 kcal/mol. If the two fragments reach a separation of 6.0 Å, we terminate the trajectory.

Because the detailed dynamical information of product is obtained at the collision energy (Ec) of 60 kcal/mol, we ran much more trajectories at Ec =60kcal/mol than those at other collision energies, for which only the total cross sections and branching ratios of the direct abstraction and roaming pathways were obtained. Specifically, a total of about 30 million trajectories were run at Ec =60kcal/mol, and roughly 1.5 million trajectories were run at the collision energies of 30 kcal/mol, 40 kcal/mol, 50 kcal/mol and 70 kcal/mol, respectively. Because the QCT calculations can result in the ZPE violation of products, the soft-ZPE constrained treatments are used to analyze the final dynamical information of products. The

soft-ZPE constrained analysis considers those trajectories in which the sum of the vibrational energies of the products is not less than the sum of the corresponding ZPEs.

In this work, two classes of trajectories that result in the H_2 + C_2H_3 product channel were observed, i.e., (i) the direct abstraction pathway via TS1 without the C_2H_5 intermediate-forming, (ii) roaming pathway via short-lived C_2H_5 adduct or long-lived C_2H_5 complex-forming. To determine whether the C_2H_5 intermediate is formed in a given trajectory, we used the following criterion. If one of the distances between the incoming H atom and two carbon atoms has at least two turning points, and there exists two local minima with the C-H distances smaller than 1.9 Å, we classify these trajectories as the C_2H_5 intermediate -forming ones. In addition, for a given C_2H_5 intermediate-forming trajectory, we found that the interval between the two hydrogen atoms leaving the carbon atom is greater than 10 fs, which can be a typical character of roaming trajectory.

SUPPLEMENTARY REFERENCES

[1] Werner, H. J., Knowles P. J., Knizia, G., Manby, F. R. & Schütz, M. Molpro: a general-purpose quantum chemistry program package. *Wiley Interdiscip. Rev. Comput. Mol. Sci.* 2012, **2**, 242–253.

[2] Werner H.-J. et al. MOLPRO, version 2012.1, a package of ab initio programs. http://www.molpro.net.

[3] Shao, K., Chen, J., Zhao, Z. & Zhang, D.H. Communication: Fitting potential energy surfaces with fundamental invariant neural network. *J. Chem. Phys.* 2016, **145**, 071101.

[4] Fu, B. & Zhang, D.H. Ab initio potential energy surfaces and quantum dynamics for polyatomic bimolecular reactions. *J. Chem. Theory Comput.* 2018, **14**, 2289-2303.

[5] Lu, X., Shao, K., Fu, B., Wang, X. & Zhang, D. H. An accurate full-dimensional potential energy surface and quasiclassical trajectory dynamics of the H + H_2O_2 two-channel reaction. *Phys. Chem. Chem. Phys.* 2018, **20**, 23095-23105.

[6] Raff, L. M., Komanduri, R., Hagan, M & Bukkapatnam, S. *Neural networks in chemical reaction dynamics*, Oxford University Press, New York, 2012.

[7] Hagan, M. T. & Menhaj, M. B., *IEEE Transactions on Neural Network*s, **5**, 989 (1994).

[8] Sarle, W. S. *Proceedings of the 27th Symposium on the Interface of Computing Science and Statistics*, 1995, 352–360.

[9] Hase, W. L. *Encyclopedia of Computational Chemistry*, ed. N. L. Allinger, Wiley, New York, 2002**, 1**, 309–407.

[10] B. Fu, B. Shepler, J. M. Bowman, Three-state trajectory surface hopping studies of the photodissociation dynamics of formaldehyde on ab initio potential energy surfaces, *J. Am.*

Chem. Soc, 2011, **133**, 7957-7968.